Materials Views
www.MaterialsViews.com

ADVANCED
MATERIALS
www.advmat.de

COMMUNICATION

Advanced Photoassisted Atomic Switches Produced Using ITO Nanowire Electrodes and Molten Photoconductive Organic Semiconductors

Annop Klamchuen, Hirofumi Tanaka,* Daisuke Tanaka, Hirotaka Toyama, Gang Meng, Sakon Rahong, Kazuki Nagashima, Masaki Kanai, Takeshi Yanagida, Tomoji Kawai, and Takuji Ogawa

Using inorganic materials to fabricate synapse-derivative devices is a very important step to produce neural computing systems. Atomic switches have attracted attention because of their synaptic-like behavior exhibiting an ability to switch on and off.[1] If photoresponsive properties can be added to atomic switches, photosensitive neuron systems such as "intelligent artificial retina devices" will be achieved in the near future. Atomic switches produced with a metal/open-gap/Ag$_2$S/ Ag structure have attracted much attention for use in ultra-high-density nonvolatile memory devices that consume low amounts of power,[1–3] because the atomic switching is performed through the formation and shrinkage of Ag conductive nanowire bridges between 1 nm-gap electrodes.[4–6] Making the gap wider and filling the gap with a functional materials such as photoconductive organic materials is a fascinating concept for achieving a functional atomic-switch device since external fields such as electric and magnetic fields could be applied to the gap, which also plays an important role in forming Ag conductive bridges.[7] We previously used *N,N*′-diheptylperylenetetracarboxylicdiimide (PTCDI), a photoconductive organic material, to demonstrate just the bridging process of a photoassisted atomic switch (PAS).[7] After bridging of the Ag wire, the junction worked as a general atomic switch. A void formed during the shrinking of the Ag conductive bridge, however, caused the degradation of PAS to suppress repeatable atomic switching because voids are difficult to repair during shrinking since PTCDI acts as a solid (melting temperature, $T_m \approx 404$ °C) in the temperature range of practical application. Thus, using both small electrodes and a photoconductive material with a lower T_m would solve this problem because it would minimize the number of voids that form and instantly repair them. Here, we report that the combination of self-assembled indium-tin-oxide (ITO) 10–20 nm-diameter nanowire electrodes and the photoconductive material, tetradodecyl perylene-3,4,9,10-tetracarboxylate (TDPC), whose $T_m \approx 79.7$ °C, was suitable to demonstrate repeatable atomic switching under light irradiation because the molecule could be melted only under light irradiation through the absorption of energy from photons. We also report that using nanowire electrodes instead of flat ones is promising for the development of various electronic nanodevices because the nanowire electrodes can confine the flowing current.[8] Furthermore, precise control of the gap size enables control of the position of small devices in integrated-circuit systems.[9] The size of gaps between the electrodes in PASs could be also controlled using vapor-liquid-solid (VLS) deposition to change the length of the ITO nanowires. Our concept of repairing voids will enable the development of the numerous integrated PASs produced with various photoconductive materials and electrode gaps of various sizes.

A photoconductive organic material was applied to the electron transport layer between two electrodes in previous PAS devices;[7] therefore, the proposed PAS does not require the short gap distance of about 1 nm, which is required for conventional atomic switches.[1,2,4] Silver sulfide (Ag$_2$S), a mixed ionic and electronic conductor, is used as the material for growing Ag conductive bridge as follows: Irradiating the photoconductive material with light and applying a positive bias to the Ag$_2$S/ Ag electrode, on the one hand, can cause photocurrent to flow between the counter and Ag$_2$S/Ag electrodes, enabling an Ag conductive bridge to grow and cross the gap. Applying positive bias to an Ag$_2$S/Ag electrode in the dark, on the other hand, does not cause an extension of an Ag conductive bridge because of the lack of photocurrent. Once the bridges are formed, the switch works as a conventional atomic switch by alternating the polarity of the applied bias voltage.[7] Although PAS devices are promising for achieving functional atomic switches, the use of the solid photoconductive material and the lithographically patterned electrode to form a ≈100 nm Ag conductive bridge may degrade the PAS because it is difficult to compensate for the formation of voids during the shrinking of Ag bridges. To solve this problem, we used TDPC, whose melting temperature is relatively low, and transparent conductive ITO nanowires as the photoconductive material and counter electrode, respectively. **Figure 1** shows the structure of a PAS device, which consists of two major parts: (1) an ITO top electrode on an ITO thin-film/glass substrate and (2) a molten photoconductive material,

Dr. A. Klamchuen, Dr. H. Tanaka,
Dr. D. Tanaka, H. Toyama, Prof. T. Ogawa
Department of Chemistry
Graduate School of Science
Osaka University
1–1 Machikaneyama
Toyonaka, Osaka, 560–0043, Japan
E-mail: tanaka@chem.sci.osaka-u.ac.jp
Dr. A. Klamchuen, Dr. G. Meng, Dr. S. Rahong,
Dr. K. Nagashima, Dr. M. Kanai, Dr. T. Yanagida,
Prof. T. Kawai
Institute of Scientific and Industrial Research
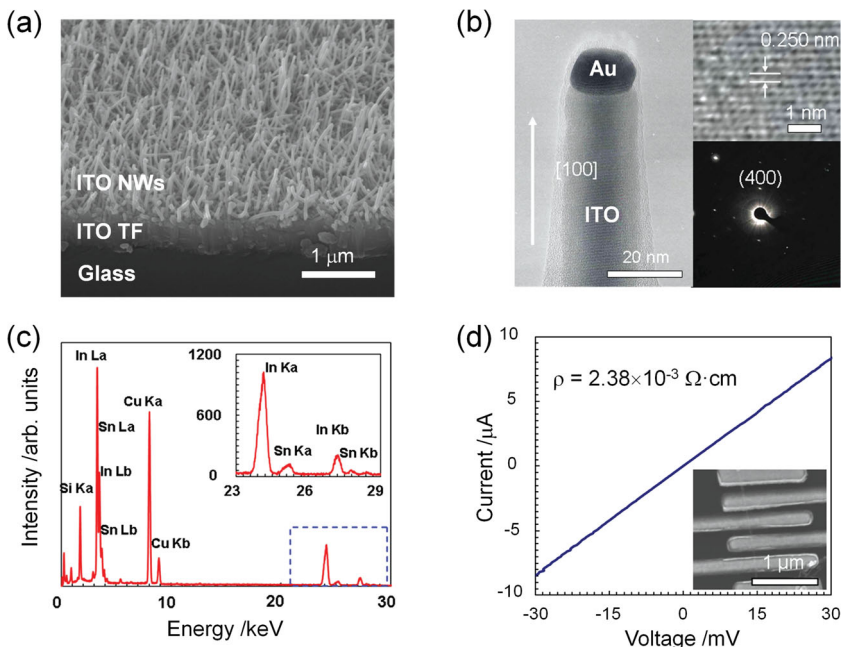Osaka University
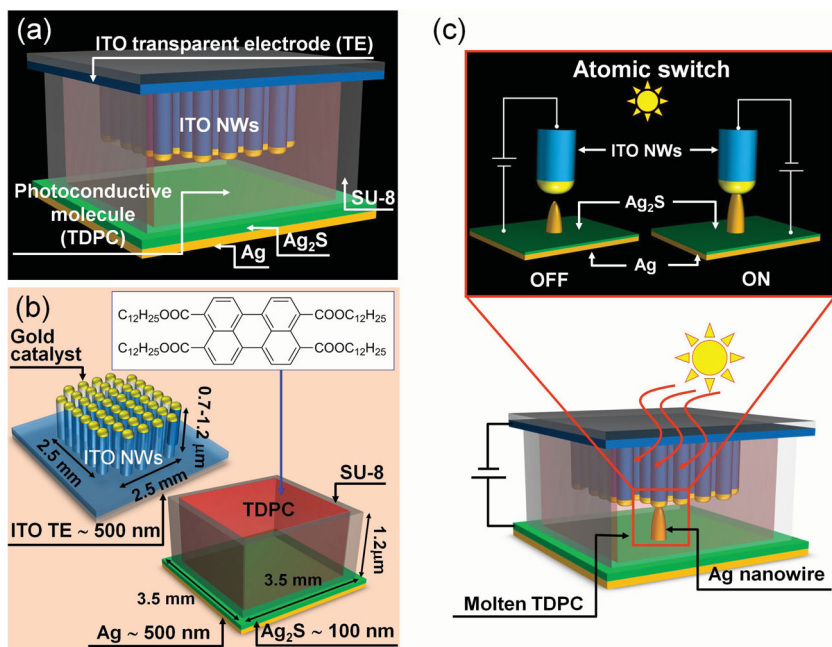
Figure 1. Schematic diagram of photoassisted atomic switch (PAS). (a) Photoconductive TDPC was sandwiched between a transparent ITO nanowire top electrode and a Ag_2S/Ag bottom electrode. (b) Structure of each electrode fabricated separately. TDPC was placed between the electrodes in a SU-8 reservoir. Gold nanoparticles remained on top of all ITO nanowires as catalyst that supported their growth. (c) PAS switching.
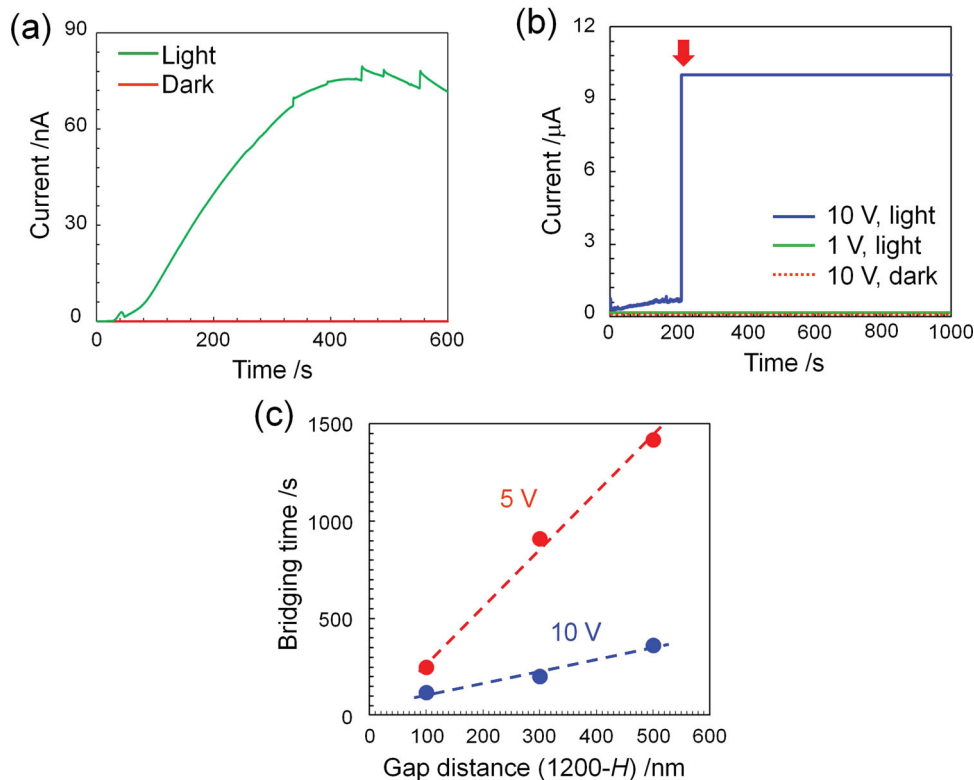
TDPC, which is contained in an SU-8 photoresist reservoir pattern on an Ag_2S/Ag electrode. The details of the fabrication of the ITO nanowire and the Ag_2S/Ag electrodes covered by photoconductive TDPC are also shown in Figure 1.

Figure 2a shows the typical field-emission scanning electron microscopy (FESEM) image of ITO nanowires grown on an ITO thin-film/glass substrate. The thickness of the ITO thin film is 500 nm and the length of the nanowires, L, are 700, 900 and 1100 nm, respectively. Note that the stated length of the ITO nanowire was obtained by averaging the lengths of 500 nanowires. The height of the most vertical nanowire, H, defines the gap size with the counter electrode. Here, H was almost identical to the same value of the length of the nanowire because of the relationship $H = L \cos\theta$ (θ, which is the angle between the wire and the normal vector to the substrate surface, is close to 0°). The growth direction is regulated by the crystal orientation of the ITO thin film on the substrate; hence, some of the nanowires were oriented at an angle with the normal vector to the substrate, so that the aforementioned gap size increased. If single-crystal ITO is used as the substrate, all the wires would be vertical with the same height,[10] but we used a polycrystalline ITO thin film in this study. Since the present work aims to demonstrate the possibility of repeating PASs switching with ITO nanowires for the future development of retina devices, we avoided using single-crystal ITO as it is expensive and unsuitable for industrial-scale production. Figure 2b shows the high-resolution transmission electron microscopy (HRTEM) image of a fabricated ITO nanowire and the corresponding selected area electron diffraction (SAED) pattern. The single crystalline nature and (100)-oriented growth of the ITO nanowire is clearly shown. The diameter of the ITO nanowire is about 20 nm. Figure 2c shows the energy-dispersive X-ray spectroscopy (EDS) data obtained during HRTEM, which was performed for an area of approximately several tens of nm^2. K-shell peaks corresponding to In and Sn are clearly observed. Note that it is crucial to identify the concentrations of In and Sn in the nanowire through the K-shell peaks rather than the L-shell peaks because of the significant overlap between the peaks associated with In and Sn. The atomic ratio of In to Sn in the nanowire was about 88.3:11.7, which is similar to that of the pellet target of pulsed laser deposition (PLD). Figure 2d shows typical current (I) versus voltage (V) data for the ITO nanowire, obtained using four-probe conductive measurement (FPCM). The inset of Figure 2d shows the FESEM image of the fabricated device structure. The resistivity of the ITO nanowire, obtained from FPCM was about 2.38×10^{-3} $\Omega \cdot cm$, indicating that the high-conductivity ITO nanowire can be used

Figure 2. Sn (10 at%)-doped In_2O_3 (ITO) nanowires. (a) FESEM image. (b) HRTEM image with SAED pattern. (c) EDS data. Inset shows magnified data around In and Sn K-shell peaks. (d) FPCM result for ITO nanowire.

Figure 3. PAS switching. (a) Photocurrent of TDPC. Red and green lines represent photocurrent measured at 1 V in darkness and under light irradiation, respectively. (b) Changes in amount of current flowing between ITO nanowires (H = 900 nm) and Ag$_2$S/Ag electrodes with TDPC intermediate layer. Dashed red line: 10 V in darkness; solid green line: 1 V under light irradiation; and solid blue line: 10 V under light irradiation. (c) Bridging times plotted as functions of gap distance.

as an electrode in atomic switch devices. Note that the resistivity of the ITO thin film is about 1.94×10^{-4} $\Omega \cdot$cm. In addition, since the diameter and length of ITO nanowires grown using VLS deposition can be controlled by controlling the size of the Au catalyst and the growth time,[11,12] it is promising that the size of the electrodes and the distance between them can be controlled using VLS deposition to grow the nanowires rather than using time-consuming and expensive electron beam lithography (EBL), which is inappropriate not only for studying PAS but also for practical device application.

Figure 3a shows the current induced in TDPC in the dark and under light irradiation. The photocurrent increased by five orders of magnitude (from 0.5 pA to 75 nA) when the TDPC was irradiated under light, indicating that TDPC is suitable for the use as a photoconductive material in PASs. Several peaks appeared around 300–600 s under light irradiation because of the change in structure during melting of TDPC. Figure 3b shows the flow of current between the Ag$_2$S and ITO nanowire electrodes measured under various conditions and plotted as functions of time. The changes in the current depended on the light irradiation condition and the bias voltage applied to the electrodes. Note that the length of the ITO nanowire is 900 nm. The results show that the current flow only changed under light irradiation when an appropriate bias voltage was applied to the electrodes, which is consistent with the results obtained for the previous PAS.[7] The amount of current when a 10 V bias voltage was applied in the dark was negligible: around 0.74 pA,

which corresponds to a resistance of 13.5 TΩ between two electrodes. However, the amount of current when irradiated under light and a bias voltage was applied gradually increased for 200 s and then rapidly increased at approximately 208 s. The current of about 729 nA (which corresponds to a resistance of 13.7 MΩ) observed at 200 s can be regarded as photocurrent due to light irradiation to the photoconductive TDPC. The sudden increase in the current from 729 nA to more than 10 μA suggests that an Ag conductive bridge contacted one of the ITO electrodes (red arrow shown in Figure 3b).[7] In other words, the current of about 729 nA facilitated the growth of the Ag conductive bridge to turn on the atomic switch. The PAS device can remain turned on even in the dark. These results highlight that the ITO nanowire and Ag$_2$S/Ag electrodes covered by the photoconductive TDPC can be used to operate PASs. Furthermore, the formation of the Ag conductive bridge requires a threshold current, shown in Figure 3b. Although the electrode subjected to a bias voltage of 1 V under light irradiation produced a photocurrent of 30 nA, which is significantly higher than the current (0.74 pA) in the dark, the PAS was not turned on. This kind of threshold current was also observed for conventional Ag$_2$S atomic switches[2,5] and in the previous study on PAS.[7] Figure 3c shows the bridging times of PAS devices plotted as functions of the size of gaps between Ag$_2$S/Ag and the ITO nanowire electrodes for the bias voltages of 5 and 10 V. The length of the nanowires was varied from 700 to 1100 nm. Note that increasing the height, H (regulated by the length of

COMMUNICATION
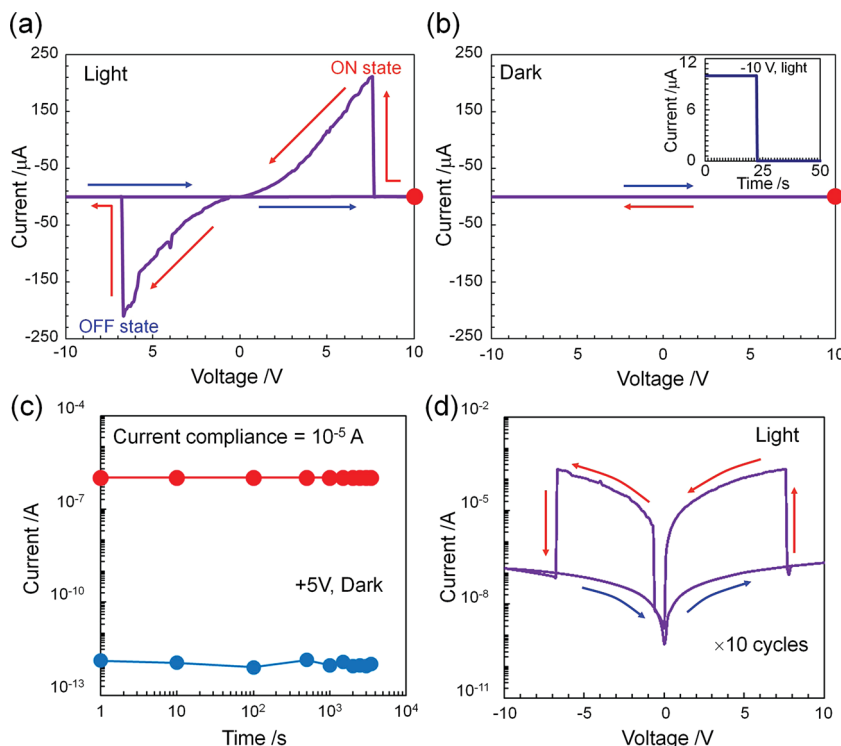
Figure 4. I–V characteristics of ITO nanowire-Ag$_2$S/Ag nanogap (H = 900 nm) electrode after initial photoassisted turn off. Arrows indicate direction of voltage sweep: Red arrows: from 10 to –10 V; Blue arrows: from –10 to 10 V. (a) Measured under light irradiation. (b) Measured in darkness. Inset of Figure 4(b) shows change in current around disconnection of Ag conductive bridge from Ag$_2$S/Ag electrode irradiated under light. Red circles in both graphs indicate starting and finishing point of bias sweeping. (c) Data-retention time of PAS switching. (d) Endurance of PAS measured under vacuum (P < 4.0 × 10^{-4} Pa) at 300 K.

the most vertical nanowire, as described above), of the ITO nanowires leads to a decrease in the size of the gaps between the ITO nanowires and the Ag$_2$S/Ag electrodes because the gap size was (1200–H) nm. The bridging time decreased with increasing H. These results indicate that the size of the gaps between the electrodes could be controlled by controlling H fabricated using VLS deposition. In addition, higher bias voltages shorten the bridging time. These findings might imply that the bridging time could be controlled by controlling the gap size and bias voltage.[7]

Next, we investigated the current-voltage (I–V) characteristics of the PAS to determine whether the switching was repeatable. It should be noted that the I–V characteristics of the PAS were observed after the Ag conductive bridge was disconnected by applying negative bias voltage to the Ag$_2$S/Ag electrode (inset of **Figure 4**b). This is because they can be used to examine the effect of the photoconductive material compensating for the voids produced during the shrinking of the Ag wire. Figure 4a shows the I–V characteristics of the PAS device irradiated under light. The I–V measurements were started when the device was turned off (i.e., at an applied bias voltage of +10 V). The length of the nanowire was 900 nm. The switch was turned on and off at about 7.7 and –6.7 V, respectively. First switching occurred at 7.7 V because the measurement was started in the OFF state, as shown in Figure S1a, Supporting Information. Figure 4c

shows the data-retention time of PAS device. The measurements were carried out at 300 K under vacuum (P < 4.0 × 10^{-4} Pa) in the dark. The readout of the currents was performed at +5 V, which was applied to Ag$_2$S/Ag electrode. It should be noted that the current compliance is limited to 10^{-5} A. ON state (low resistance state) and OFF state (high resistance state) of the PAS device is maintained for at least 3600 s, clearly indicating that our device can act as nonvolatile memory device. Figure 4d shows the continuous switching event of the PAS device. The observed switching cycle is 10 times under light irradiation. The switch was turned ON and OFF at approximately 7.7 and –6.7 V, respectively. The ON/OFF ratio is about 10^5 to 10^6. These results confirmed that our PAS device is stable and capable o provide continuous switching. Reproducibility was checked by performing measurements on five samples. The hysteric I–V characteristic repeatedly observed was similar to that exhibited by conventional atomic switches.[2,4–6] The off-resistance of 43 GΩ and on-resistance of 36 kΩ between the two electrodes during repeated operation produced a sufficiently high on/off ratio (10^6). These results highlight that using molten photoconductive material and nanoelectrodes might be responsible for the stable PAS event because of the absence of voids during the shrinking of the Ag conductive bridge. Furthermore, the switching event with the same device could not be observed in the dark, as shown in Figure 4b. The resistance between the two electrodes was about 1.94 TΩ, which seemed to make it difficult to grow and shrink the Ag conductive bridge. This result means that switching Figure 4a can only occur under light irradiation as described above. This behavior is totally different from that of conventional atomic switches. The result also implies that the disconnection of the Ag conductive bridge through the negative bias applied at the initial state provided sufficient distance to suppress switching under the low amount of current flowing between the electrodes, which has never been observed in previous PAS devices.[7] Switching was again observed when the electrodes were irradiated under light. Since controlling the formation and shrinkage of the Ag conductive bridge at both the initial state and switching required the electrodes to be subjected to a bias voltage and irradiated under light, the introduction of various molten photoconductive materials with different absorption wavelengths into the gap between the ITO nanowire and the Ag$_2$S/Ag electrode to obtain functional atomic-switch devices that exhibit wavelength-selected photoassisted atomic switches could be achieved in the near future. Thus, integrating the synaptic memory of conventional atomic switches with PAS devices produced with various photoconductive materials is a promising method of developing photosensitive neuron systems such as intelligent artificial retina devices.

Materials Views
www.MaterialsViews.com

ADVANCED
MATERIALS
www.advmat.de

COMMUNICATION

We used self-assembled ITO nanowires as transparent nanoelectrodes to demonstrate stable PAS events. The organic molecule, TDPC, was used as an alternative molten photoconductive material. A stable PAS switching could only be demonstrated under light irradiation. These results highlight that using nanoelectrodes and molten photoconductive material is a promising method for preventing the formation of voids during the shrinking of the Ag conductive bridge. We also found that the length of the ITO nanowires played a crucial role in the switching behavior of the PAS. Our concept enables the development of a wide range of PAS nanodevices such as an intelligent artificial retina device that exhibits wavelength selectivity and nonvolatile memory.

Experimental Section

Au-catalyst-assisted PLD (ArF excimer laser, λ = 193 nm) was used to grow high-density ITO nanowire electrodes in a 2.5×2.5 mm^2 area on an ITO thin film/glass substrate.[11] A pellet consisting of a mixture of In and Sn powders (Kojundo Chemical Laboratory Co., Ltd.) was used as the target, and the ratio of the concentration (at%) of Sn to In was constantly maintained at 10:90. Details about the growth and characterization of the ITO nanowires can be found elsewhere in the literature.[12] The length, L, of the nanowires was varied from 700 to 1100 nm, and the diameter of the nanowires was 20 nm. The Ag$_2$S/Ag electrode was prepared using an electron beam evaporation system (Canon ANELVA Corporation L-045E) to deposit a Cr/Ag (10 nm/100 nm) thin film onto a SiO$_2$/Si substrate, then, the surface was sulfurized by following a modified procedure reported earlier.[13] The substrate was dipped into an 0.1%-Na$_2$S aqueous solution for 12 h at room temperature. The photoconductive material, TDPC, was synthesized according to literature procedures.[14] SU-8 photoresist and photolithography were used to fabricate the reservoir pattern for containing the molten TDPC on the Ag$_2$S/Ag electrode in order to produce the device structure. The reservoir pattern size was 3×3 mm^2, and the depth was 1.2 μm. A molten photoconductive TDPC contained in the SU-8 photoresist was then sandwiched between an ITO nanowire electrode and an Ag$_2$S/Ag counter electrode under heating at 80 °C. The gap between the ITO nanowire electrode and the Ag$_2$S/Ag electrode was controlled by controlling the length of the nanowires. The time dependence of the current and the I–V characteristics were measured with an Advantest R6245 2-channel I–V source monitor interfaced to a computer through a GPIB-SCSI board according to the NI-488.2 protocol. The measurement data were collected using a homemade procedure and Igor Pro 4.0 (WaveMetrics) software. The light was irradiated using a MAX-303 ASAHI spectra Xenon lamp with a band-pass filter in the range 300–600 nm. All measurements were performed under high vacuum (P < 4.0×10^{-4} Pa) at 300 K.

Supporting Information

Supporting Information is available from the Wiley Online Library or from the author.

[1] T. Ohno, T. Hasegawa, T. Tsuruoka, K. Terabe, J. K. Gimzewski, M. Aono, *Nat. Mater.* **2011**, *10*, 591.

[2] K. Terabe, T. Hasegawa, T. Nakayama, M. Aono, *Nature* **2005**, *433*, 47.

[3] I. Valov, I. Sapezanskaia, A. Nayak, T. Tsuruoka, T. Bredow, T. Hasegawa, G. Staikov, M. Aono, R. Waser, *Nat. Mater.* **2012**, *11*, 530.

[4] K. Terabe, T. Nakayama, T. Hasegawa, M. Aono, *J. Appl. Phys.* **2002**, *91*, 10110.

[5] T. Hino, T. Hasegawa, K. Terabe, T. Tsuruoka, A. Nayak, T. Ohno, M. Aono, *Sci. Technol. Adv. Mater* **2011**, *12*, 013003.

[6] A. Nayak, T. Tamura, T. Tsuruoka, K. Terabe, S. Hosaka, T. Hasegawa, M. Aono, *J. Phys. Chem. Lett.* **2010**, *1*, 604.

[7] T. Hino, H. Tanaka, T. Hasegawa, M. Aono, T. Ogawa, *Small* **2010**, *6*, 1745.

[8] a) D. W. M. Arrigan, *Analyst* **2004**, *129*, 1157; b) J. Hees, R. Hoffmann, A. Kriele, W. Smirnov, H. Obloh, K. Glorer, B. Raynor, R. Driad, N. J. Yang, O. A. Williams, C. E. Nebel, *Acs Nano* **2011**, *5*, 3339.

[9] a) L. E. Jensen, M. T. Bjork, S. Jeppesen, A. I. Persson, B. J. Ohlsson, L. Samuelson, *Nano Lett.* **2004**, *4*, 1961; b) A. I. Persson, L. E. Froberg, S. Jeppesen, M. T. Bjork, L. Samuelson, *J. Appl. Phys.* **2007**, *101*, 034313.

[10] Q. Wan, P. Feng, T. H. Wang, *Appl. Phys. Lett.* **2006**, *89*.

[11] a) K. Nagashima, T. Yanagida, H. Tanaka, T. Kawai, *J. Appl. Phys.* **2007**, *101*, 124304; b) A. Marcu, T. Yanagida, K. Nagashima, H. Tanaka, T. Kawai, *J. Appl. Phys.* **2007**, *102*, 016102; c) T. Yanagida, A. Marcu, H. Matsui, K. Nagashima, K. Oka, K. Yokota, M. Taniguchi, T. Kawai, *J. Phys. Chem. C* **2008**, *112*, 18923; d) A. Marcu, T. Yanagida, K. Nagashima, K. Oka, H. Tanaka, T. Kawai, *Appl. Phys. Lett.* **2008**, *92*, 173119; e) K. Nagashima, T. Yanagida, A. Klamchuen, M. Kanai, K. Oka, S. Seki, T. Kawai, *Appl. Phys. Lett.* **2010**, *96*, 073110.

[12] a) A. Klamchuen, T. Yanagida, K. Nagashima, S. Seki, K. Oka, M. Taniguchi, T. Kawai, *Appl. Phys. Lett.* **2009**, *95*, 242902; b) A. Klamchuen, T. Yanagida, M. Kanai, K. Nagashima, K. Oka, S. Seki, M. Suzuki, Y. Hidaka, S. Kai, T. Kawai, *Appl. Phys. Lett.* **2011**, *98*, 053107.

[13] S. Saitoh, Y. Araki, M. Taira, *Dent. Mater. J.* **2006**, *25*, 316.

[14] S. Benning, H. S. Kitzerow, H. Bock, M. F. Achard, *Liq. Cryst.* **2000**, *27*, 901.